AD-A160 408 EYE MOVEMENTS AND SPATIAL PATTERN VISION(U) EYE 1/1
RESEARCH INST OF RETINA FOUNDATION BOSTON MA L E AREND
28 FEB 85 AFOSR-TR-85-0741 F49620-83-C-0052

UNCLASSIFIED F/G 6/16 NL

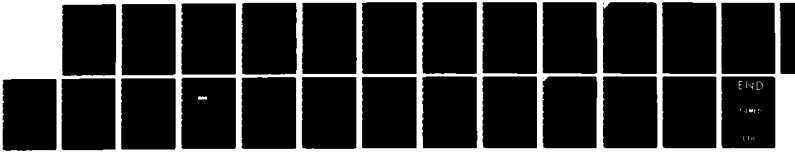

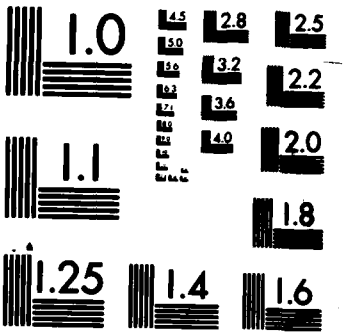

UNCLASSIFIED

SECURITY CLASSIFICATION OF THIS PAGE (When Data Entered)

REPORT DOCUMENTATION PAGE	READ INSTRUCTIONS BEFORE COMPLETING FORM
1. REPORT NUMBER AFOSR-TR- 85-0741	2. GOVT ACCESSION NO. / 3. RECIPIENT'S CATALOG NUMBER
4. TITLE (and Subtitle) EYE MOVEMENTS AND SPATIAL PATTERN VISION	5. TYPE OF REPORT & PERIOD COVERED Annual Report 2/1/84 - 1/31/85
	6. PERFORMING ORG. REPORT NUMBER
7. AUTHOR(s) Dr. Lawrence E. Arend	8. CONTRACT OR GRANT NUMBER(s) F49620-83-C-0052
9. PERFORMING ORGANIZATION NAME AND ADDRESS Eye Research Institute 20 Staniford Street Boston, MA 02114	10. PROGRAM ELEMENT, PROJECT, TASK AREA & WORK UNIT NUMBERS 2313/A5 61102F
11. CONTROLLING OFFICE NAME AND ADDRESS Air Force Office of Scientific Research/NL Bolling AFB, DC 20332-6448	12. REPORT DATE 28 Feb 85
	13. NUMBER OF PAGES 22
14. MONITORING AGENCY NAME & ADDRESS(if different from Controlling Office)	15. SECURITY CLASS. (of this report) Unclassified
	15a. DECLASSIFICATION/DOWNGRADING SCHEDULE

16. DISTRIBUTION STATEMENT (of this Report)

Approved for public release;
distribution unlimited.

17. DISTRIBUTION STATEMENT (of the abstract entered in Block 20, if different from Report)

18. SUPPLEMENTARY NOTES

19. KEY WORDS (Continue on reverse side if necessary and identify by block number)

Eye Movements, Spatial Pattern Vision, Stabilized Retinal Images, Visual Illusions, Brightness Constancy, Color Constancy.

20. ABSTRACT (Continue on reverse side if necessary and identify by block number)

Low contrast, low spatial frequency luminance sawtooth patterns look like luminance staircases, with no brightness changes over the shallower luminance slope. Brightness measurements at corresponding points in different cycles of these patterns showed substantial illusory brightness differences. Other measurements showed that the illusion is not confined to

DD FORM 1 JAN 73 1473 EDITION OF 1 NOV 65 IS OBSOLETE

UNCLASSIFIED

SECURITY CLASSIFICATION OF THIS PAGE (When Data Entered)

Annual Technical Report
F49620-83-C-0052
28 February 1985

EYE MOVEMENTS AND SPATIAL PATTERN VISION

Dr. Lawrence E. Arend

Eye Research Institute
20 Staniford Street
Boston, MA 02114

Controlling Office: Air Force Office of Scientific Research/NL
Bolling AFB, DC 20332-6448

REPORT: 2/1/84 TO 1/31/85

I. OBJECTIVES

The overall objective of the project is further development of a model (Arend, 1973) describing the role of retinal image motion in the human visual system's processing of edge information in patterns. Several lines of investigation were proposed, including:

A. Eye Movements and Stabilized Retinal Images

Recent experiments using grating patterns held stationary on the retina have raised questions concerning the role of retinal image motion in spatial pattern vision. The fact that high contrast gratings remain visible when stabilized with the SRI Double Purkinje Image Eyetracker (Kelly, 1979) has been interpreted as meaning that the human visual system can process pattern information in the absence of temporal change of the retinal image, contradicting previous views. This issue is a critical part of the most basic understanding of human pattern vision. A goal of the second year of the project was completion of stabilization work in which we 1) replicated Kelly's basic observations of stabilized gratings and 2) reinterpreted all grating stabilization data in light of new calculations of the sensitivity of the human visual system to small image motion.

B. Spatial Gradients and Integration over Edge Information

A large component of the project is investigation of how information from sharp and shallow spatial gradients of intensity and color gets assembled into a stable and reliable visual array of lightness and color. Second year goals for this portion of the project were 1) completion and calibration of the display system consisting of minicomputer, image processor and color video monitor 2) software development for displaying patterns and controlling experiments and 3) preliminary experiments on gradient illusions.

II. STATUS OF RESEARCH EFFORT

A. Stabilized Retinal Images

Substantial progress was made in evaluating Purkinje Image Eyetracker stabilization of gratings. The principal conclusions are:

1) Most of the gross form of Kelly's grating stabilization data replicates in our lab using a similar eyetracker, different subjects and improved methods.

2) Calculations from stabilized grating contrast sensitivities show that the P.I. tracker (in fact, probably no existent eyetracker) can eliminate all meaningful retinal image motion and therefore:

a) Residual visibility of stabilized objects does not necessarily imply that the visual system contains mechanisms capable of responding to temporally unchanging inputs and
b) Only subjective pattern fading and disappearance can be relied upon as a criterion of stabilization adequacy, and then only with qualification.

In light of current evidence, therefore, it is likely that all pattern information is derived from retinal temporal changes, and some model describing the extraction of spatial pattern information from temporal information is required. The only current model with such a mechanism is Arend's (1973).

At the beginning of the year we replicated with a second subject our stabilized contrast sensitivity data using the reduced exposure techniques of Burbeck and Kelly (1984) (described in detail in first year report). A manuscript describing all of the stabilized grating experiments and the motion-sensitivity calculations was prepared and submitted to the Journal of the Optical Society of America.

B. Spatial Gradients and Integration of Edge Information

1. Display System. During the first year a display system consisting of a VAX 11/750 minicomputer, an Adage 3000 image processor and a Tektronix 690 RGB monitor was selected, purchased, and installed. The display system was calibrated in the second year to provide accurate specification of luminance and chromaticity over the full output range of the monitor.

The spectral emitances of the red, green, and blue phosphors of the monitor were obtained by a grating-monochromator multichannel analyzer and the CIE chromaticity coordinates of the phosphors were calculated (fig. 1).

Luminance vs. digital-input-data curves were obtained for the three guns singly and together at nine screen locations. Unlike published data on other monitors (Cowan, 1984) the curves for all three guns were well fit by a single power function (after multiplication by a constant equating the maximum outputs for the guns). Thus the outputs can all be linearized with one power function. The function in use linearizes the light output to better than one percent at all values (fig. 2). The output of the phosphors is stable; repeatability is excellent from week to week.

The principle limitation of the display system in its current form is the AC coupling of the monitor. While the output is accurately clamped to a constant reference level at the beginning of each horizontal sweep the output drifts slightly within the sweep in a manner which depends on the intensity at the beginning of the sweep. The effect is small (>5%), but may prove to be a significant limitation in work with high contrast patterns. Given the otherwise highly satisfactory performance of

Figure 1. Relative power spectra of phosphors of Tektronix 690 monitor. Right peak: red phosphor. Middle peak: green phosphor. Left peak: blue phosphor.

Fig. 2. a) Luminance of Tektronix 690 phosphors as function of digital data applied to D/A converters. Scaled to maximum luminance of white (all three guns at maximum)=94.0 Cd/m^2. Curves, top to bottom: white (all guns on), green, red, blue.

b) Curves of fig. 2a each scaled to its own maximum luminance. Power function is the same for all three guns.

c) Luminance curves of phosphors after linearization, as function of image data level. Each curve scaled to its own maximum.

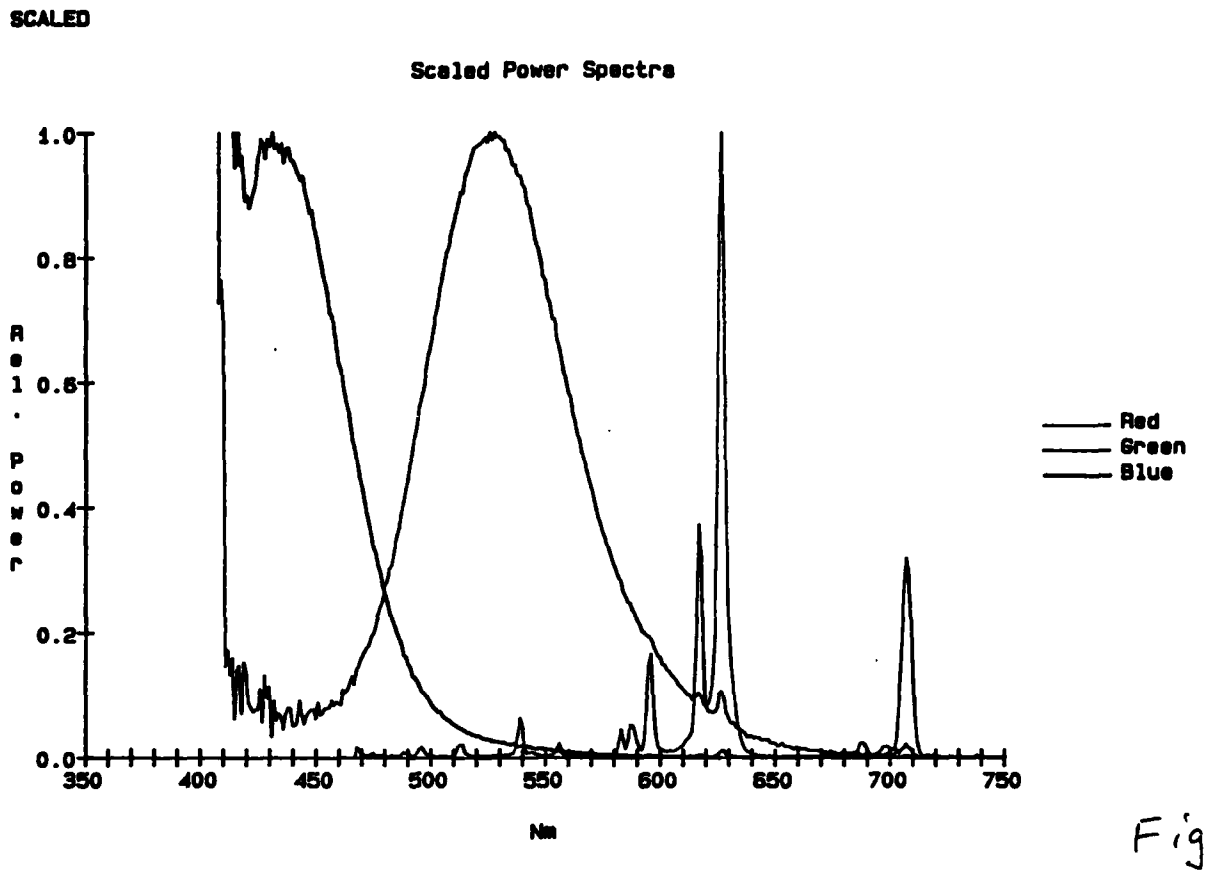
SCALED
Scaled Power Spectra
1.0
0.8
0.6
0.4
0.2
0.0
Rel. Power
350
400
450
500
550
600
650
700
750
Nm
Red
Green
Blue

Fig. 1

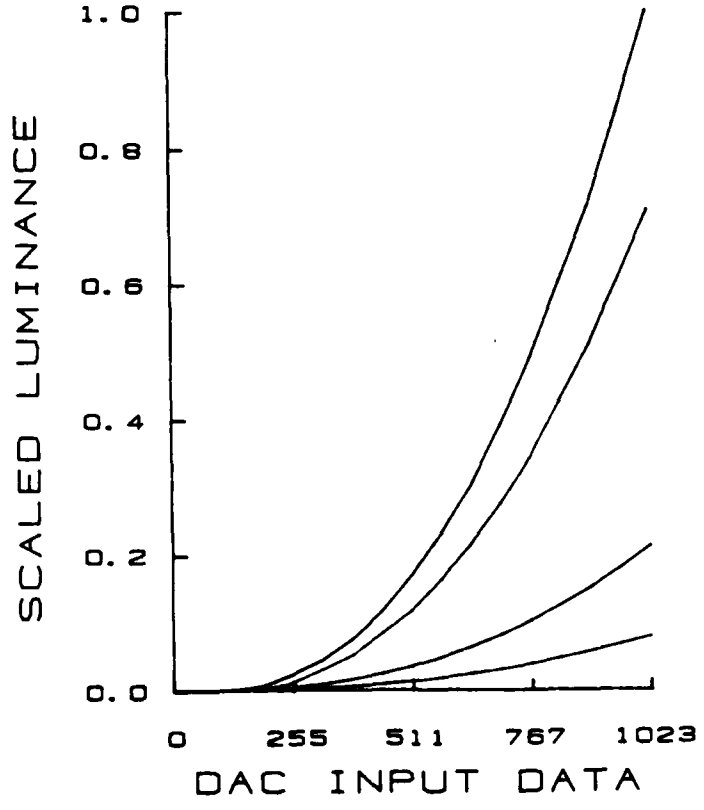
1.0
0.8
0.6
0.4
0.2
0.0
SCALED LUMINANCE
0
255
511
767
1023
DAC INPUT DATA

Fig. 2a

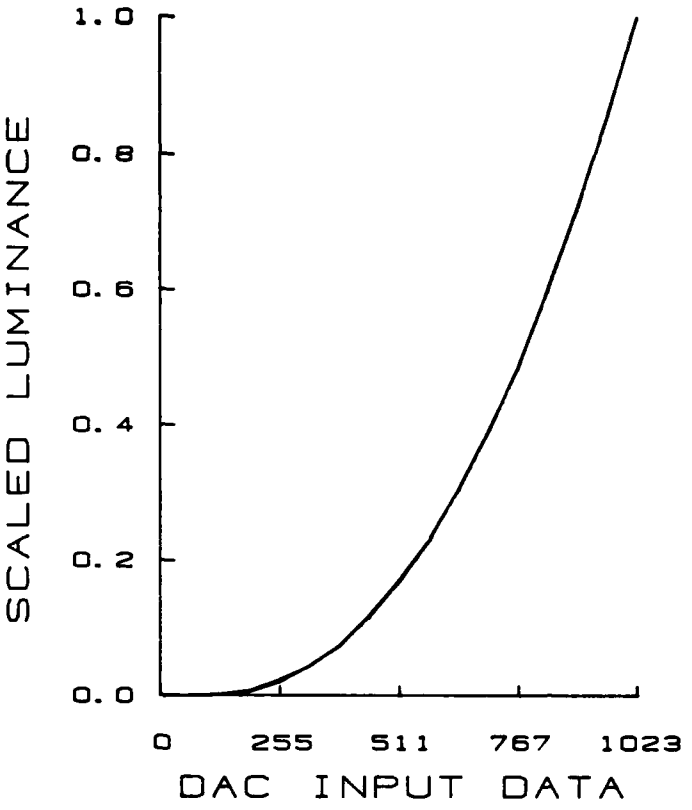
1.0
0.8
0.6
0.4
0.2
0.0
SCALED LUMINANCE
0
255
511
767
1023
DAC INPUT DATA

Fig. 2b

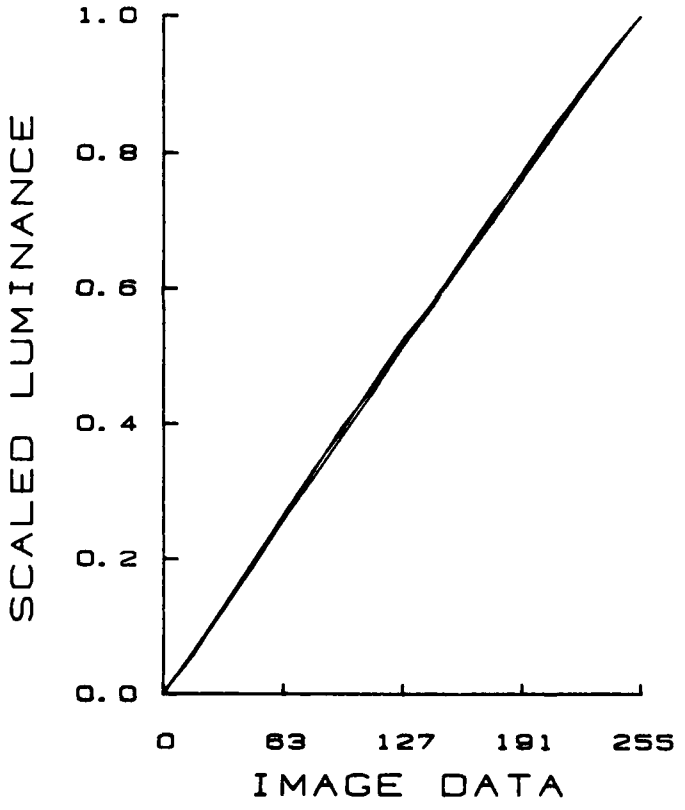
1.0
0.8
0.6
0.4
0.2
0.0
SCALED LUMINANCE
0
63
127
191
255
IMAGE DATA

Fig. 2c

Figure 3. Luminance and brightness as a function of radial distance. Inset: display configuration. Left: luminance along radius of inset (zero = center). Right: sketch of brightness distribution along radius of inset pattern. Subject adjusted luminance of rectangle in inset pattern to match brightness at points 1 and 2.

Figure 4. Brightness matches for patterns of fig. 3 as a function of pattern contrast $(=(L_{max}-L_{min})/(L_{max}+L_{min}))$. Circles, top: point 1, top configuration of fig. 3. Circles, bottom: point 2, top configuration. Squares, top: point 2, bottom configuration of fig. 3. Squares, bottom: point 1, bottom configuration. Subject LA.

Figure 5. Same as fig. 4, subject RG.

Figure 6. Estimates of percentage of width of band which appeared uniform in brightness as a function of pattern contrast. Patterns of fig. 3, top configuration. Circles: outer band. Squares: inner band. Subject LA.

Figure 7. Same as fig. 6, subject RG.

the display, modifications to provide DC coupling will be deferred until the need is clearly demonstrated.

2. Measurement of Gradient Illusions. The first step in studying gradient illusions (Craik-O'Brien-Cornsweet and related illusions) was development of satisfactory techniques for measuring the appearance of these complex spatial patterns.

We explored several techniques and used them to obtain more quantitative detail than previously available A wide variety of shallow gradient patterns yield illusory brightnesses. We chose initially to study a circular ring pattern with a radial luminance distribution consisting of three cycles of a low contrast sawtooth (fig. 3). Even though the three cycles have identical luminance the figure appears as a nearly uniform brightness central disk surrounded by two nearly uniform rings of increasing (3a) or decreasing (3b) brightness relative to the central disk.

The subject could vary the luminance of a small square in the corner ofthe display to make its brightness match the centers of the inner and outerbands (fig. 3, 1 and 2).

In figs. 4 and 5 are brightness matches from two subjects for several sawtooth contrasts in each polarity. While there are important differences of detail the subjects generally agree that substantial brightness differences occurred at all contrasts. This was a somewhat surprising result. In the simplest form of the model the illusory brightness differences require that the shallow gradient be below threshold and not perceived. At our lowest contrast the bands were very uniform in brightness and the edges had low apparent contrast. At the highest physical contrast the rings had pronounced brightness gradients between high contrast edges. It was initially somewhat surprising therefore that large brightness differences occurred even in the presence of the visible gradient. In an attempt to quantify the appearances at the various contrasts the subjects were asked to judge the fraction ofthe ring which appeared uniform in brightness. While there are obviously criterion definition problems with this task, in practice the judgements were not difficult and had reasonable error bars. Means of five judgements are shown in figs. 6 and 7. Both subjects judged the lowest contrast patterns to have only narrow regions of nonuniformity adjacent to the contours. At the highest contrast both saw brightness gradients over most of the ring, but RG adopted a less strict criterion than LA.

Upon closer consideration there are two simple possible explanations for the the brightness differences at the highest constrasts: 1) Even though less of each ring appears uniform, the uniform portion spans a greater luminance range due to the higher physical contrast. 2) The threshold for gradient need not be a step function wherein increases of luminance gradient change abruptly from no visibility to weight equal to that given steep gradients; a more reasonable function would be sigmoid with physical gradients passing gradually from no representation of shallow gradients through progressively greater weights for steeper gradients. While the second option seems likely, the data in figs. 4-7 are also consistent with the first.

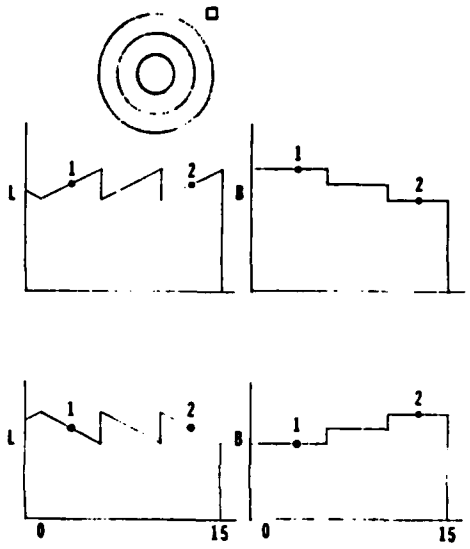

Fig. 3

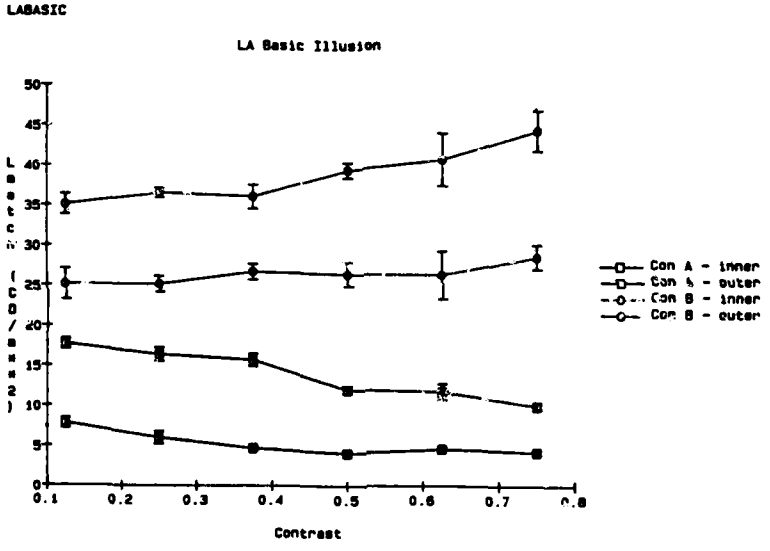

Fig. 4

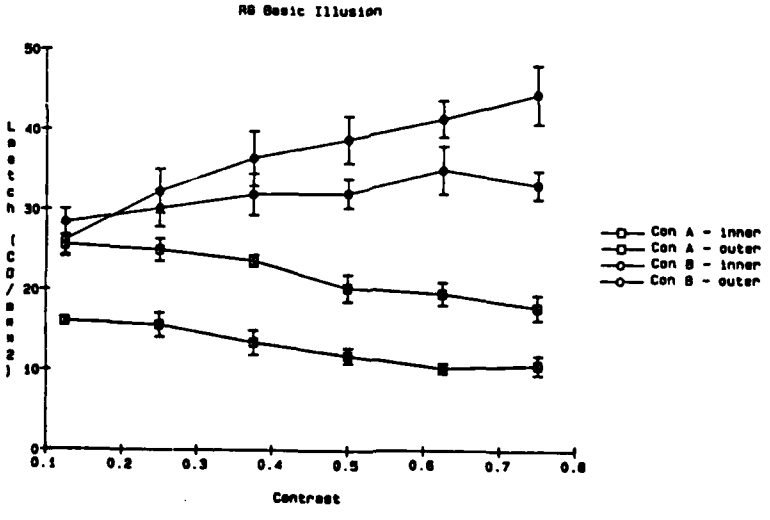

Fig. 5

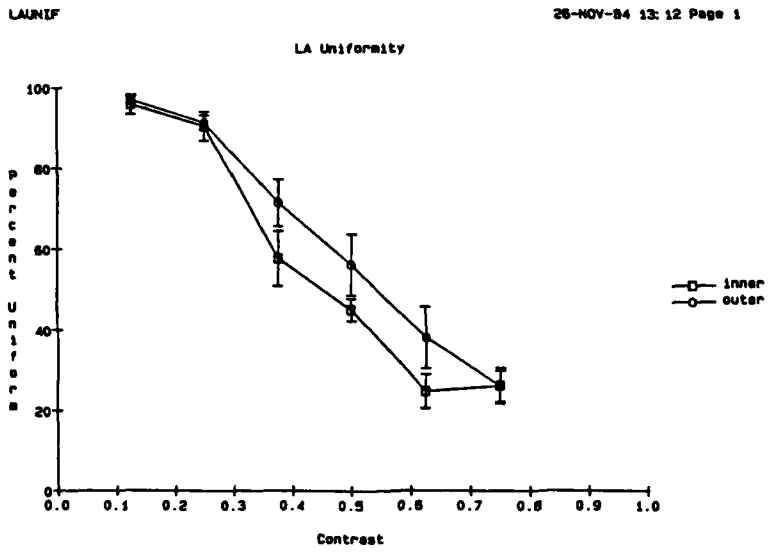
LAUNIF
26-NOV-84 13: 12 Page 1
LA Uniformity
percent Uniform
100
80
60
40
20
0
0.0
0.1
0.2
0.3
0.4
0.5
0.6
0.7
0.8
0.9
1.0
Contrast
inner
outer

Fig. 6

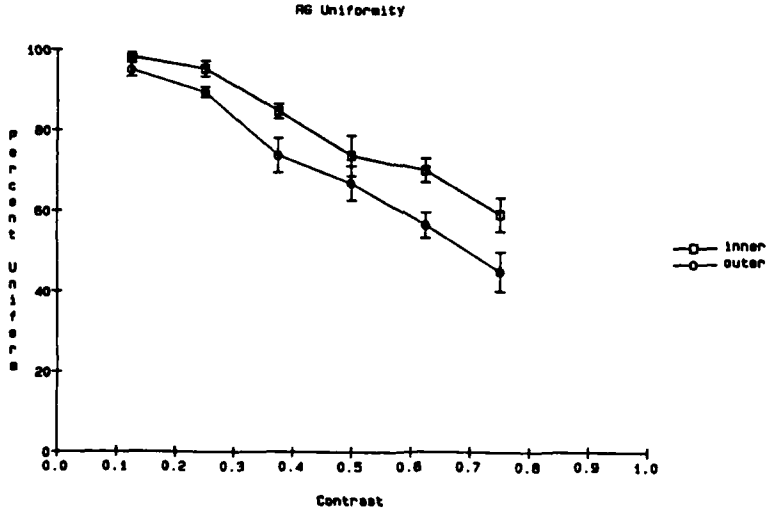
RG Uniformity
percent Uniform
100
80
60
40
20
0
0.0
0.1
0.2
0.3
0.4
0.5
0.6
0.7
0.8
0.9
1.0
Contrast
inner
outer

Fig. 7

The graded threshold account is, however, supported by a further experiment. Patterns with the radial luminance profiles of fig. 8 have no subthreshold gradients if the small steps are detectable. Nevertheless, for patterns with many small steps per ring there is a clear brightness difference between the bands. In fig. 9 are brightness matching data from two subjects for 5-11 steps per ring. In all the stimuli the small steps were visible. No brightness differences occurred for few steps, but clear differences occurred at 9 and 11 steps. The brightness differences in fig. 9 clearly indicate that the sum of the small brightness steps within the rings did not equal the sum of the large brightness steps between rings. We therefore conclude that the threshold for spatial gradient is not abrupt but graded. More detailed experiments will allow determination of the form of the weighting curve transferring luminance gradients to brightness gradients.

3. Gradient and Curl A major issue proposed for second and third year study was inconsistent integrals in two dimensional applications of Land and McCann's (1971) and Arend's (1973) essentially one-dimensional models. The problem is illustrated in fig. 10. According to both models the brightness of B relative to that of A is obtained by the visual system by taking the gradient of log retinal illuminance, setting all gradients below some threshold to zero and integrating over the resulting distribution. Explicitly in Land and McCann's model and implicitly in Arend's the differentiation and integration are done along arbitrarily chosen curves between A and B. The models make the correct prediction along the straight line joining A and B in fig. 10. The shallow gradient is below threshold so the only derivatives going into the integral are the downward steps at the contours, indicating that B is darker than A. Along the path crossing the outer boundary, however, we get a different answer. There is no change between A and the outer boundary, a downward step of known magnitude to the background luminance, no change over the background segment, an upward step on crossing back into B's band equal and opposite to the initial crossing into the background, and no change between the outer boundary and B. The sum of these derivatives is zero indicating that A and B are equal in brightness.

These inconsistent integrals will occur with any model which accounts for gradient illusions by taking derivatives or differences, thresholding, and then summing or integrating. This includes second-derivative models like Horn (1974) and Marr's (1974). In all cases the presence of path-dependent line integrals means there is no true two-dimensional integral and some special process must be proposed for resolving the inconsistencies (unless one wishes to propose that the appearance of such patterns is unstable or multistable, changing over time, or perhaps beyond description at any given time).

Not all patterns produce inconsistent integrals in the models. The radial sawtooth distributions of fig. 3, for example, produce no inconsistent integrals. All paths between a point in the inner ring and a point in the outer ring cross the same subthreshold and suprathreshold gradients. It seemed

Figure 8. Cube root of luminance as function of radial position.

Figure 9. a) Brightness matches of centers of three bands of pattern of fig. 8 as function of pattern contrast (same definition as fig. 4). Top curve: inner band. Middle curve: middle band. Bottom curve: outer band. Subject AR.

b) Same as fig. 9a, subject LA.

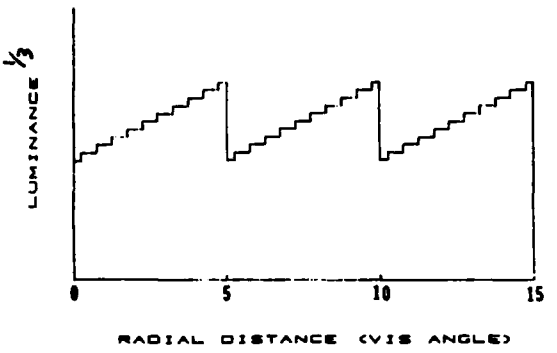

Fig. 8

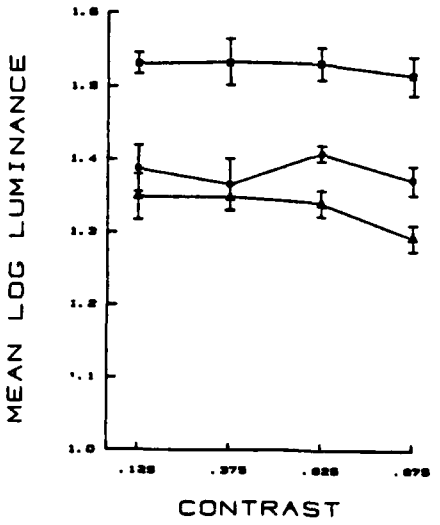

Fig. 9a

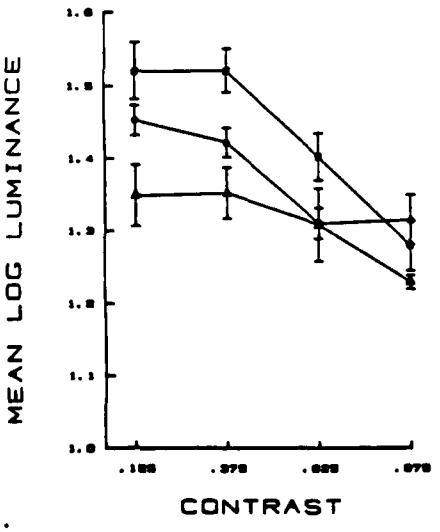

Fig. 9b

Figure 10. Schematic of integrals computed in brightness models along various paths through two sawtooth luminance patterns. a) Left panel: Linear sawtooth pattern. Right panel: Sketch of integral of thresholded derivative along paths 1 and 2 between points A and B. b) Left panel: Radial sawtooth pattern. Right panel: Sketch of integral of thresholded spatial derivative of luminance along paths 3 and 4 between points C and D. Shallow luminance gradient is below threshold, abrupt steps are not.

Figure 11. Display for brightness matches to half of radial sawtooth pattern. Subject adjusts luminance of rectangle to match brightness of center of inner ring or outer ring.

Figure 12. Brightness matches of centers of rings of radial sawtooth luminance patterns as function of luminance of surround (L_{max}=94.0 Cd/m^2). a) Complete pattern. Squares: inner ring. Circles: outer ring. b) Half pattern. Squares: inner ring. Circles: outer ring. Subject LA.

Figure 13. Same as Fig. 12, subject RG.

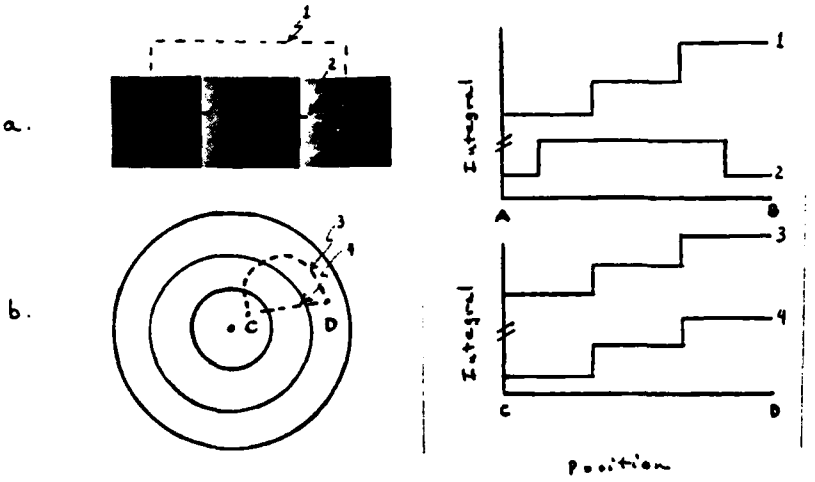

Fig. 10

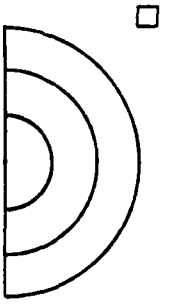

Fig. 11

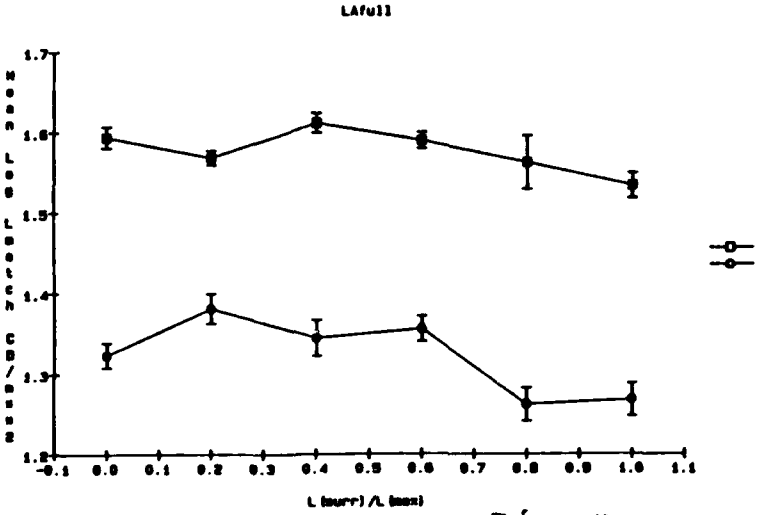

Fig. 12a

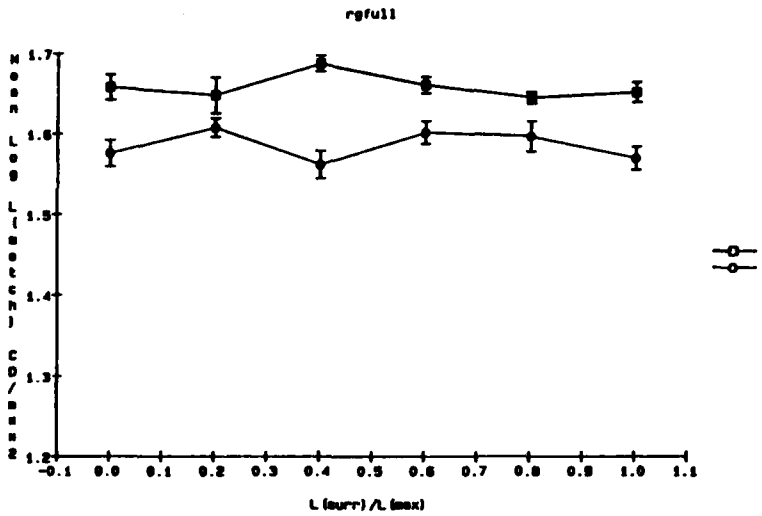

Fig. 13a

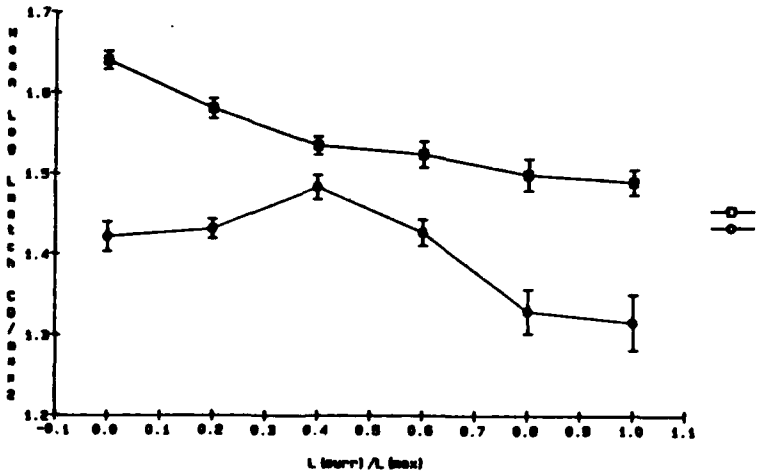

Fig. 12b

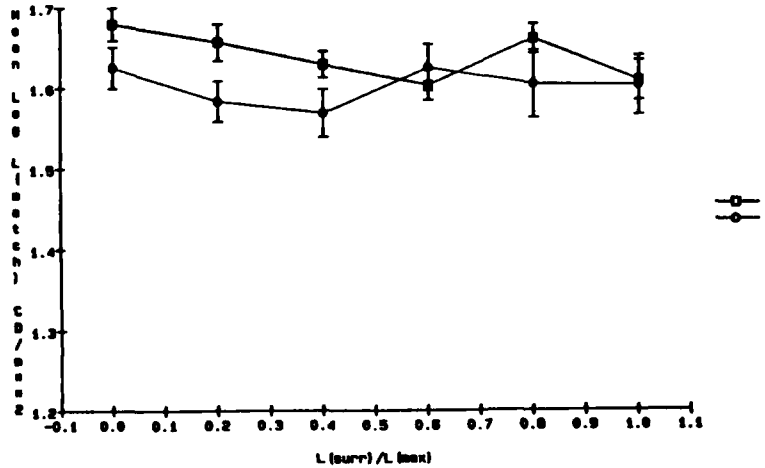

Fig. 13b

possible that distributions with inconsistent integrals might produce smaller illusory brightness differences and larger brightness gradients than consistent patterns. To test this hypothesis we matched brightnesses in radial-sawtooth disks (see fig. 4) and radial-sawtooth half disks (fig. 11). The latter are merely curved versions of the pattern in fig. 10 and have the same inconsistent integral problems. Data from two subjects are shown in figs. 12 and 13. As hypothesized the half-disk brightness difference (and hence the size of the illusion) is consistently smaller than for the full-disk for both subjects. The difference is less pronounced for RG than for LA, and background luminance had a larger effect on LA's half-disk data than RG's.

Analysis of inconsistent integral problems led us to two new paradoxical patterns, the circumferential sawtooth pattern and the drifting sawtooth illusion.

As noted in the original proposal, one way of resolving the problems in the integration is to perceive brightness gradients which reduce or remove the curl responsible for the inconsistent integrals, i.e., essentially, lower one's threshold for the spatial luminance gradients. While no quantitative data have yet been collected documenting the appearance of the full and half ring patterns, their appearances are consistent with this type of solution. Brightness gradients are much more pronounced in the half-ring patterns than in the corresponding full-ring patterns.

There is, however, at least one other method of resolving the problem. The offending curl occurs where the border with the background slices across the subthreshold luminance gradient as, for example, at the top and bottom of fig. 10. If the integration is carried out only over areas which do not cross this border there are no inconsistent integrals. Thus the problem could be dealt with by segmenting the visual field into separate areas of integration, each internally consistent. The visual problem then reduces to combining the output of the separate integrations to give a brightness distribution extending over the entire visual field. This segmentation could resemble the segmentation required for veridical perception of areas under very different illuminations.

Some evidence that the visual system is sensitive to the geometrical relations among subregions of the image comes from observations of "circumferential sawtooths", displays with a sawtooth luminance distribution around a circumference rather than along a radius (fig. 14). In this distribution a line integral extending from point A around the circumference back to A is not zero (indicating that A is brighter than A or that A is darker than A, depending on the direction of rotation). Visually this pattern is unstable (or possibly multistable) with the brightness distribution varying from moment to moment, depending upon such factors as eye movements and point of fixation. Two adjacent sectors frequently look different in brightness and relatively homogeneous within sectors (though never as homogeneous as in the bands in fig. 3 even when the luminance gradient is less). The other two sectors, however, are nonuniform and their brightness relative to the other three

Figure 14. Luminance as a function of angular position in annular circumferential sawtooth pattern. Dashed line: path of problematic integral of thresholded spatial derivative of luminance in brightness models. Shallow gradient within sectors is below threshold, abrupt steps are not. Thus integral after 360^{o} counterclockwise rotation is sum of four downward steps, indicating that brightness of A does not equal brightness of A.

Figure 15. Sketch of truncated circumferential sawtooth pattern.

Figure 16. CIE diagram indicating Red/Green isoluminous gratings of saturation CSF experiment. Closed curve: spectrum locus. Triangle: color space of Tektronix monitor, corners are phosphor loci. Upper point: experimentally determined unique green. Lower point: D_{6500} white of monitor. Gratings were formed by modulating sinusoidally as indicated in the figure along the line passing through unique green and D_{6500}.

Figure 17. Logarithm of inverse of excitation purity of green peak of just detectable isoluminous chromaticity grating as function of spatial frequency.
Purity = (green peak - D_{6500})/(510 nm - D_{500})

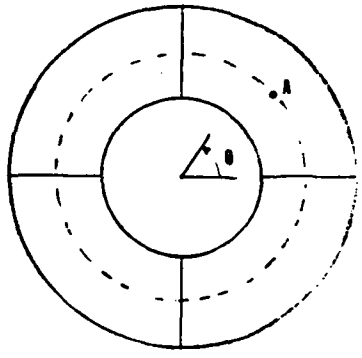

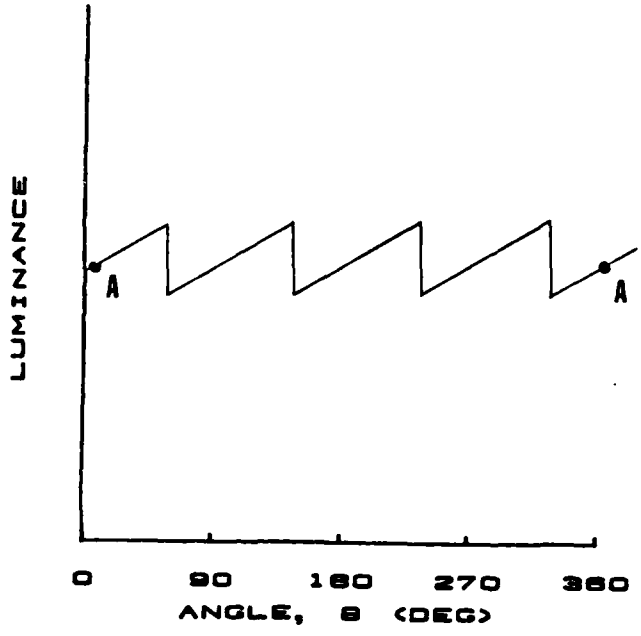

Fig. 14

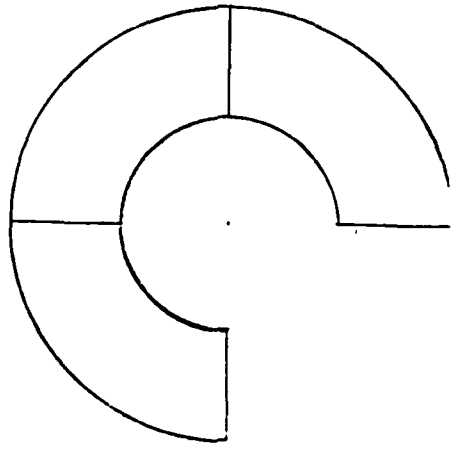

Fig. 15

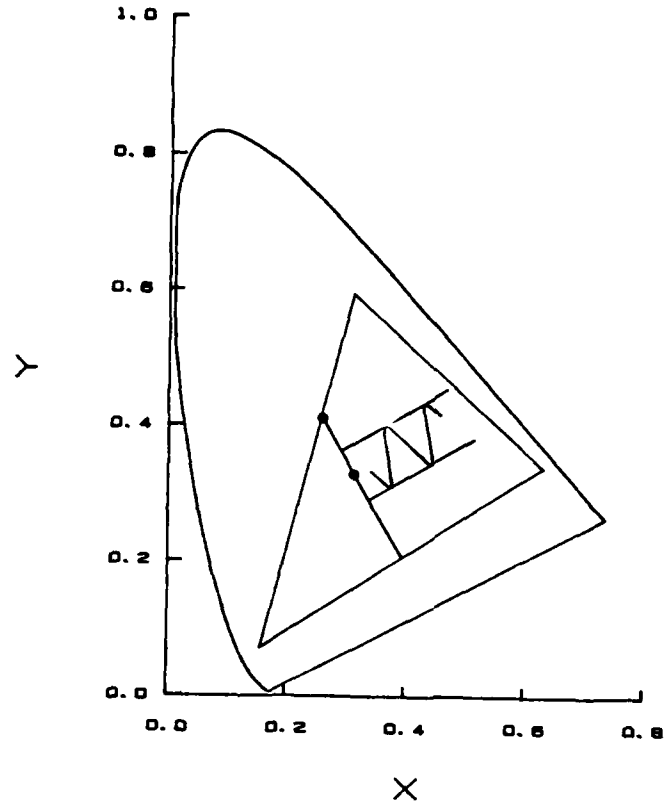
1.0
0.8
0.6
0.4
0.2
0.0
Y
0.0
0.2
0.4
0.6
0.8
X

Fig. 16

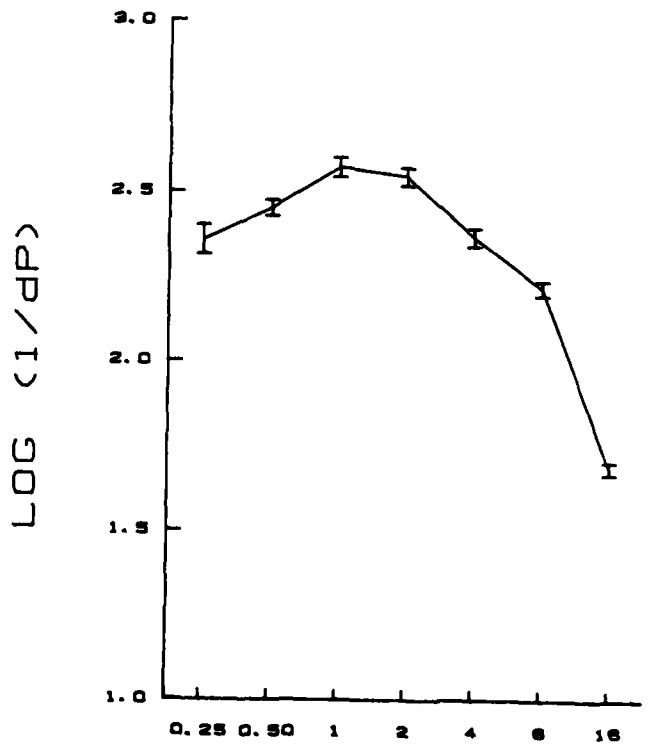
3.0
2.5
2.0
1.5
1.0
LOG (1/dP)
0.25
0.50
1
2
4
8
16
SPATIAL FREQUENCY

Fig. 17

sectors remains vague, even under close attention. If one sector is now replaced by the dark background there is still curl at the inner and outer borders of each sector (fig. 15). Nevertheless, the three remaining sectors immediately appear uniform and different in brightness.

We have also discovered a remarkable illusion in which stripes successively drift onto the display, each stripe darker than the previous, but with no change in the overall brightness of the display. Two cycles of a low contrast luminance sawtooth initially fill the screen, appearing quite homogeneous with the left brighter than the right. The entire pattern is then slowly drifted to the left with new cycles of sawtooth appearing on the right edge to replace the portions disappearing at the left. Each cycle as it appears is darker than those to its left. Under passive viewing there is no obvious change in the brightness of the band as it moves across the screen, giving the overall impression that darker bars are being added to the screen. It is only with mental effort that one notices that the overall brightness of the screen is not changing. Under careful scrutiny the brightness of the individual cycle can be seen to increase during its traverse.

These experiments with inconsistent integral patterns provide further demonstrations that the visual system represents patterns not in terms of local luminances or luminance ratios, but in terms of relatively global integrals over spatial derivative information.

4. Chromatic CSF's A third line of investigation proposed for years two and three is obtaining further data on spatial color mechanisms. Measurement of spatial chromatic contrast sensitivity functions about a number of points in color space was proposed, eventually extending to suprathreshold contrast matching functions as well as threshold functions. The mean chromaticities and modulation axes in color space are to be chosen to modulate either within or across opponent color systems.

A first isoluminous CSF has been measured, modulating about the D6500 alignment white of the monitor, modulating along the line indicated in fig. 16. The modulation line passes through our experimentally determined unique green (using the D6500 white as the adaptation stimulus) and the D6500 white locus. Constant luminance was obtained by selecting two lights the same short distance on either side of D6500. The lights were then displayed as the two halves of a 2° split disk, with the subject adjusting the luminance of one side to minimize the border between the hemidisks. This equal luminance criterion has been shown to give results similar to flicker photometry. The maximum contrast chromatic grating for the experiment is formed by sinusoidally modulating along the line between these two lights. Data fo. one subject are shown in fig. 17, plotted in terms of the excitation purity (re D6500 and the unique green spectrum intercept) of the green peak of the just-detectable grating.

These experiments have just begun, but several features agree with previous work. Van der Horst and Bouman (1969) found in similar experiments a slight peak at 1 c/deg with very little (continued on next page)

decline at low spatial frequencies (their lowest spatial frequency was 0.7 c/deg). Our peak is at 1 c/deg, but there is a clear low frequency decline, as in Kelly's (1981) chromatic CSF's (Kelly modulated around a yellow). Our sensitivity declines more slowly at high spatial frequencies than van der Horst and Bouman's.

REFERENCES

Arend, L. E. (1973) Spatial and differential operators in human vision. **Psychol. Rev., 80,** 374-395.

Cowan, W.B. (1984) An inexpensive scheme for calibration of a colour monitor in terms of CIE standard coordinates. Computer Graphics and Applications, In Press.

Horn, B. K. P. (1974) Determining lightness from an image. Computer Graphics and Image Processing, 3, 277-299.

Van der Horst, G. J. C. and Bouman, M. A. (1969) Spatiotemporal chromaticity discrimination. J. Opt. Soc. Amer., 59, 1482-1488.

Kelly, D. H. (1979) Motion and Vision. II. Stabilized spatiotemporal threshold surface. J. Opt. Soc. Amer., 69, 1340-1349.

Kelly, D. H. (1981) Disappearance of stabilized chromatic gratings. Science, 214, 1257-1258.

Land, E. H. and McCann, J. J. (1971) Lightness and Retinex theory. J. Opt. Soc. Amer., 61, 1-11.

Marr, D. (1974) The computation of lightness by the primate retina. Vision Research, 14, 1377-1388.

III. PAPERS IN PREPARATION

Arend, L. E. and Timberlake, G. T. Stabilized Gratings: Do sustained psychophysical detectors exist? Submitted to J. Opt. Soc. Amer.

Arend, L. E. and Lange, R. V. Apparent contrast of suprathreshold spatiotemporal gratings. (Probably to be submitted to Vision Research).

Arend, L. E. Shallow gradient illusions. (Probably to be submitted to Vis. Res.)

Arend, L.E. Inconsistent integrals in gradient illusions. (Probably to be submitted to Vision Research).

IV. PROFESSIONAL PERSONNEL

Arend, Lawrence E., Principal Investigator

Timberlake, George T., nonsalaried part-time collaborator

Lange, Robert V., nonsalaried part-time collaborator

V. PROFESSIONAL TALKS PRESENTED

Brown University, Psychology Department Colloquium, "Inconsistent integrals in brightness illusions", November, 1984.

Visual Information Processing Research Review, AFOSR, "Stabilized Retinal Gratings", May, 1984.

END

FILMED

11-85

DTIC